

신경망을 이용한 감지기의 고장발견, 확인 및 보완에 관한 연구

안영환*

Application of Neural Networks to Sensor Failure Detection, Identification, and Accommodation

Younghwan An*

ABSTRACT

감지기의 고장 발견, 확인, 보완은 복잡한 항공 시스템의 중요한 문제로 부각되어 왔으며, 그동안 칼만 필터를 이용한 기존 추정기술 혹은 온라인 학습 인공지능 알고리즘 등이 이 같은 문제를 해결하기 위해 제시되어 왔다. 본 연구에서는 여분의 감지기가 없는 항공제어계에 대해 온라인 학습 신경망을 이용한 감지기의 고장 발견, 확인, 그리고 보완에 관해 초점을 둔다. 이 내고장성 항공제어계는 주 신경조직망과 n 개의 국소 신경조직망으로 이루어지는데, 포괄적인 감지기의 고장을 발견하는 능력을 가진다. 어떤 경우에는 기존의 감지기 고장 발견 방법이 미세한 감지기 고장의 경우, 감지기 고장을 발견하지 못하기 때문에, 감지기 고장 발견 방법의 성능을 향상시키기 위해 수정된 감지방법이 소개되고 그 보완된 감지방법을 이용하여 기존의 방법과 성능비교가 이루어졌다.

Key Words : Sensor failures (감지기의 고장), On-line learning neural networks (온라인 학습 신경망), Failure detection (고장 발견), Fault tolerance (내고장성)

1. INTRODUCTION

Much emphasis has been currently placed on the design of fault tolerant flight control systems for low weight and unmanned aerial vehicles (UAVs) used for remote sensing purposes. Also, the relatively low procurement of high performance military aircraft along with the cancellation of plans for building new aircraft has renewed interest toward fault tolerant flight control system. In general, a fault tolerant flight control system is required to perform^(1,5):

-Sensor failure detection, identification, and

accommodation (SFDIA);

-Actuator failure detection, identification, and accommodation (AFDIA);

Particularly, the SFDIA task can be divided into :

-Sensor failure detection and identification (SFDI), which monitors the degree of deterioration in the accuracy of the sensors.

-Sensor failure accommodation (SFA), which replaces the faulty sensor with an appropriate estimator.

This paper is specifically related to fault tolerant capabilities following sensor failures using an analytical redundancy approach. Such an approach, which is

* West Virginia University, 기계항공과

more appealing approach when weight optimization is of main concern, consists of the use of state estimation schemes capable of replacing a faulty sensor. The importance of the added safety achievable through the implementation of these artificial intelligence schemes is obvious, especially for unmanned aircraft.

This paper presents the results of a SFDIA scheme with a detection technique modified with respect to a previous scheme^(1,6). The paper is organized as it follows. The next section reviews the NN-based SFDIA scheme, followed by a section describing the results of the simulations for sensor failures, particularly small bias with slowly drifting sensor failure. A final section summarizes the paper with conclusions.

2. NEURAL NETWORK-BASED SFDIA SCHEME

Sensor failure detection and identification (FDI) is an important issue, particularly in the case when the measurements from a failed sensor are used in the feedback loop of a control law. Theoretical FDI techniques, such as Generalized Likelihood Ratio and Multiple-Model Kalman Filtering, etc., perform a continuous measurements from the sensors^(3,4). At nominal conditions these signals follow some known patterns with a certain degree of uncertainty due to system and measurement noises. However, when sensor failures occur, the measurements deviate from the predictable trajectories computed on-line or off-line from state estimation schemes.

The main problems associated with the application of these failure detection schemes are their suitability limited to linear time invariant systems and their applicability only when system model is identical to filter or observer model. As an alternative approach, the implementation of Neural Networks (NNs) in flight control laws, that is sensor/actuator failure detection, identification, and accommodation (S/AFDIA), has been proposed and developed in recent years^(1,2,5)

To date, the Standard Back-Propagation Algorithm (SBPA), a gradient-based optimization method, has been widely used as a training algorithm for the NN architecture. However, there are some drawbacks such as learning speed and local minimums associated with the SBPA^(7,8).

These problems may be solved by introducing a

heterogeneous network, meaning that each neuron in the hidden and output layer of the NN has the capability of updating the output range (upper and lower bounds U, L) and the slope of the sigmoid activation function (T) as given by

$$f(x, U, L, T) = \frac{U - L}{1 + e^{-x/T}} + L \quad (1)$$

where x is the same argument as in the SBPA sigmoid activation function. This learning algorithm has been named the Extended Back-Propagation Algorithm (EBPA) and has demonstrated substantial performance improvements with respect to the SBPA in terms of accuracy and learning speed⁽⁹⁾.

Using on-line learning NN estimators, the overall SFDIA problem can be solved by introducing multiple NN architectures. The scheme consists of a main NN and a set of n decentralized NNs, where n is the number of the sensors in the flight control system without physical redundancy. The outputs of the MNN are the predictors of the state at time 'k' using measurements from 'k-1' to 'k-l' to be compared with the actual measurement at time 'k'. For the i-th of the n DNNs the output is the on-line prediction of the measurement of the i-th sensor, that is, the prediction of the state at time 'k' using measurements from 'k-1' to 'k-l' to be compared with the actual measurement at time 'k'.

In the original SFDIA scheme, when the MNN quadratic estimation error (MQEE) exceeds some predefined threshold, the scheme deduces that a sensor failure may be occurring or has already occurred. Following the positive sensor failure detection, the learning for each DNN is stopped and the DNN quadratic estimation error (DQEE) exceeding, at the same time instant, another threshold at the i-th DNN provides the identification. Then, for the accommodation phase, the i-th DNN output is used as input to the MNN in order to allow the MNN to still able to provide detection until the end of the flight and to any other DNN that use i-th sensor as an input parameter.

The following quadratic parameter, the sum of difference between the actual data from the sensors (Y) and the estimates from the MNN (O), is used for sensor failure detection (SFD) purposes :

$$MQEE(k) = \frac{1}{2} \sum_{i=1}^{\text{Num.of DNNs}} (Y_i(k) - O_{i,MNN}(k))^2$$

$$= \frac{1}{2} \left[(p(k) - \hat{p}_{MNN}(k))^2 + (q(k) - \hat{q}_{MNN}(k))^2 + (r(k) - \hat{r}_{MNN}(k))^2 \right] \quad (2)$$

The sensor failure identification (SFI) can instead be achieved by monitoring the absolute value of the estimation error of each DNN, defined as

$$DQEE_x(k) = \frac{1}{2} (x(k) - \hat{x}(k))^2 \quad (3)$$

where x = p, q, and r

For sensor failure accommodation (SFA) purposes, the following classic parameters for the estimation error are instead evaluated:

$$DAEE_x = \frac{1}{N} \sum_{k=1}^N (x(k) - \hat{x}(k)) \quad (4)$$

$$DVEE_x = \frac{1}{N} \sum_{k=1}^N [(x(k) - \hat{x}(k)) - DAEE_x]^2$$

where x = p, q, and r (5)

where DAEE and DVEE represent the DNN estimation error mean and variance respectively. The 'N' refers to the number of time steps from the instant when failure of sensor is declared to the end of the simulation.

In the case of a step-type sensor failure, the desirable detection capabilities are provided by the peak value of the MQEE parameter regardless of bias magnitude. However, in the case of soft sensor failures, particularly for ramp-type sensor failures, the MQEE-criterion has not shown reliable detection capabilities⁽⁶⁾. Therefore, a modification has been introduced to provide desirable performance under conditions resulting from any type of failures. This modified SFDIA scheme makes use of a different NN quadratic estimation error defined by :

$$OQEE(k) = \frac{1}{2} \sum_{i=1}^{\text{Num.of DNNs}} (O_{i,MNN}(k) - O_{i,DNN}(k))^2$$

$$= \frac{1}{2} \left[(\hat{p}_{MNN}(k) - \hat{p}_{DNN}(k))^2 + (\hat{q}_{MNN}(k) - \hat{q}_{DNN}(k))^2 + (\hat{r}_{MNN}(k) - \hat{r}_{DNN}(k))^2 \right] \quad (6)$$

where \hat{p}_{DNN} , \hat{q}_{DNN} , and \hat{r}_{DNN} are the estimates of p, q, and r from the respective DNNs.

The need for the use of this new parameter for SFD purposes is better described by an analysis of a typical sensor failure. For example, when a pitch rate gyro fails, the three parameters q(k), $\hat{q}_{MNN}(k)$, and $\hat{q}_{DNN}(k)$ within the 'MQEE' and 'OQEE' are considered. At nominal conditions $\hat{q}_{MNN}(k)$ and $\hat{q}_{DNN}(k)$ are estimated by the MNN and q-DNN respectively to emulate the actual pitch rate gyro. In the event of a ramp-type q-gyro failure, the \hat{q}_{MNN} tends to resemble the corrupted signals from the gyro. In fact, since the pitch rate gyro is included as the input parameter in MNN (see Table 1), the MNN architecture is updated with the failed q-gyro values during the on-line learning.

Table 1 Architecture for the MNN and q-DNN

	Main NN	q-DNN
Input parameters	I_{MNN}	I_{q-DNN}
Data pattern	5	5
Total inputs	25	20
Hidden layer	1	1
Neurons in HLs	25	20
Outputs	$\hat{p}, \hat{q}, \hat{r}$	\hat{q}
Learning rate	0.01	0.01
Momentum coef.	0.005	0.005
PTBU ¹	784	504

$$I_{MNN} = p, q, r, \phi, \theta$$

$$I_{q-DNN} = \alpha, a_n, a_x, \dot{w}$$

¹Number of parameters to be updated at each iteration for NN in the on-line learning mode

As a result, MQEE does not provide an accurate detection because the difference between q(k) and $\hat{q}_{MNN}(k)$ is relatively small despite the gyro failure. However, the output of the q-DNN ($\hat{q}_{DNN}(k)$) in Eq.(6) follows the nominal 'q' value (that is the value as it would be without a failure) relatively well despite the sensor failure. This is because the q-DNN does not receive, as input data, measurements from the faulty sensor, as shown in Table 1. The discrepancy between \hat{q}_{MNN} and \hat{q}_{DNN} in Eq.(6) causes, therefore, the peak of 'OQEE'. This problem does not occur for the step-type sensor failures. In fact, for these failures

$\hat{Q}_{MNN}(k)$ is not consistent with the measurement from the failed sensor, which induces therefore a peak for MQEE. In general, MQEE provides better performance for step-type sensor failures whereas OQEE performs better for ramp-type of sensor failures. The results of comparative studies for these detection scheme are shown in the following section.

3. ANALYSIS OF THE ON-LINE LEARNING SFDIA SCHEME

The mathematical aircraft model of this simulation is a B747-200, which is representative of a large four jet-engine commercial transport airplane⁽¹⁰⁾. Elevators, ailerons, and a vertical rudder are the primary control surfaces. In this study, the SFDIA scheme is used only for failures related to the roll rate (p), pitch rate (q), and yaw rate (r) gyros due to their importance in the aircraft feedback control laws. Therefore, for the NN-based SFDIA scheme there is one MNN, which is always in the learning mode, and three DNNs. The architectures for the MNN and q-DNN are shown in Table 1. The numerical simulation starts at typical cruise conditions, defined by an altitude of 12,192 m and at an airspeed of 265 m/sec.

A generic angular gyro accuracy is characterized by two factors: drift and scale factor. Since gyro drift appears as an additive term on the gyro output, sensor failure can be modeled as

$$X_{failure,i} = X_{nom,i} + \rho n_i \quad (7)$$

where n_i is the direction vector for the i-th faulty sensor, and ρ is the magnitude of the failure which can be positive or negative. In addition, system imperfections can cause variations in the scale factor which appear as a factor at the output of the gyro. Therefore, sensor failure can be modeled as,

$$X_{failure,i} = (1.0 + k n_i) X_{nom,i} \quad (8)$$

where k is an amplitude for the i-th faulty sensor. According to the direction vector, n_i , sensor failure can be modeled as:

- for step-type sensor failures, $n_i = 1$;

- for ramp-type sensor failures,

$$n_i = \frac{t - t_{f1}}{t_{f2} - t_{f1}} \quad (t_{f1} \leq t \leq t_{f2})$$

$$n_i = 1 \quad (t \geq t_{f2})$$

where t_{f1} and t_{f2} indicate the initial and final time instant of ramp-type sensor failure, respectively. The different types of sensor failures considered in this study based on the above formula are represented by :

Type #1 : Large sudden bias (< 5 deg/sec);

Type #2 : Small sudden bias (< 1.5 deg/sec);

Type #3 : Large bias with fast transient period (< 1 sec);

Type #4 : Small bias with slow transient period (< 5 sec);

Table 2 Detection time between two parameters

	MQEE	OQEE	MQEE+OQEE
Type#1	50.00 ¹ (50.00)	50.02 (50.02)	50.00 (50.00)
Type#2	50.48 (50.48)	50.52 (50.50)	50.48 (50.48)
Type#3	- (-)	50.48 (50.16)	50.48 (50.16)
Type#4	- (-)	53.90 (53.76)	53.90 (53.76)

¹ Additive sensor failure detection time

() : Multiplicative sensor failure detection time

- : No sensor failure declared

An on-line learning process is simulated following 30,000 sec of off-line training. A maneuver lasting 100 sec is then flown for each rate gyro failure case with the sensor failure occurring at exactly 50 sec. The results of the comparative studies between two detection parameters for the pitch rate gyro failure are shown in Table 2 and 3. A careful analysis of these results reveals the following conclusions.

From Table 2, it can be seen that MQEE-criterion provides quicker detection in comparison with the OQEE-criterion for the step-type sensor failure (type#1,2) regardless of the magnitude of bias. Clearly, a larger sudden bias induces a larger MNN error spike and the failure is declared instantaneously at 50 sec for type#1 and at 50.48 sec for type#2 depending on the size of the rate gyro DNN error. When the SFDIA is successful, the values of MQEE should go back to extremely low values as soon as the faulty q sensor is

replaced by the estimate from the q-DNN. For the ramp bias, sensor failure was modeled by type#3 and #4. It should be noticed that in none of the type#3/#4 (large/small bias with fast/slow ramp) the MQEE-criterion triggers the detection and the successive accommodation. However, the OQEE-criterion provides a reliable detection capability to SFDIA scheme due to the difference of outputs error between MNN and DNNs. From the results presented in Table 2, the MQEE-criterion seems more suitable for step-type sensor failures while the OQEE-criterion performs better for ramp-type sensor failures. Thus, a 'double detection trigger' (MQEE and/or OQEE) can provide desirable performance for any sensor failure type.

Table 3 Comparative studies for estimation error in terms of variance for the pitch rate gyro

	MQEE	MQEE+OQEE
Type#3	0.0211 ¹ (0.3072)	0.0065 (0.0058)
Type#4	0.0092 (0.3086)	0.0069 (0.0105)

¹: Additive sensor failure case

(): Multiplicative sensor failure case

Table 3 shows the result of a comparative study using estimation error in terms of variance between 'MQEE' and 'OQEE' detection criterion for the ramp bias sensor failures. These values were computed from the instant after the failure occurrence to the end of simulation. Since the first criterion does not trigger a detection of failure for the small/large bias with slow/fast ramp, it may not make sense to talk about estimation error mean and variance during the SFA for the case when 'MQEE' is used alone. However, it is important to recognize how much the estimators deviate from the nominal sensor values when the first criterion does not provide a failure detection or even a timely failure detection. The failure-declared time of the second criterion is used in the comparative study. From the results presented in Table 3, the modified detection technique shows improved performance in terms of estimation variance.

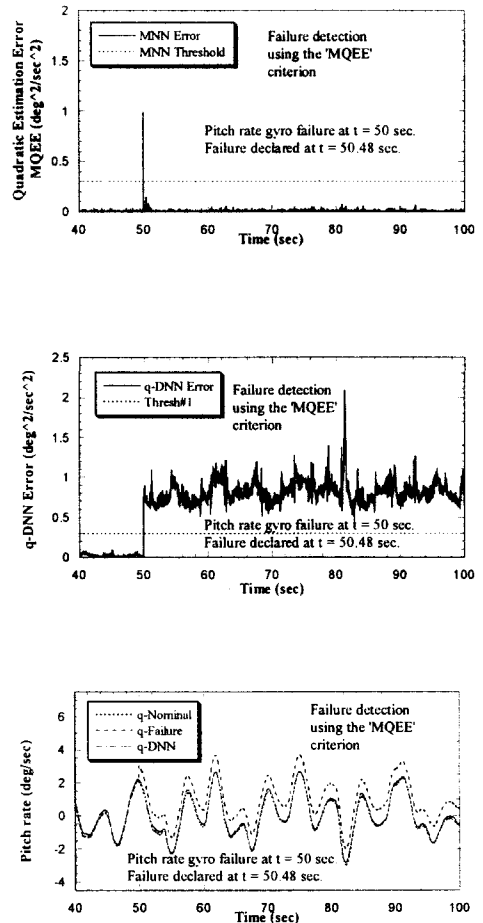


Fig. 1(a,b,c) SFDIA process for the additive step-type pitch rate gyro failure (Type #2)

Some graphical results of this comparative studies are shown in Figs. 1-5 where only the results of type #2 and #4 sensor failure are plotted. These types of failures are selected because they are believed to be the worst case scenario. This soft failure may not degrade the system performance for the time after its occurrence but, if left uncompensated, can lead the system to critical and, eventually, catastrophic conditions. In the case of step-type sensor failure (Type#2) from Fig. 1, the SFD is achieved by MQEE criterion, followed by successful identification and accommodation.

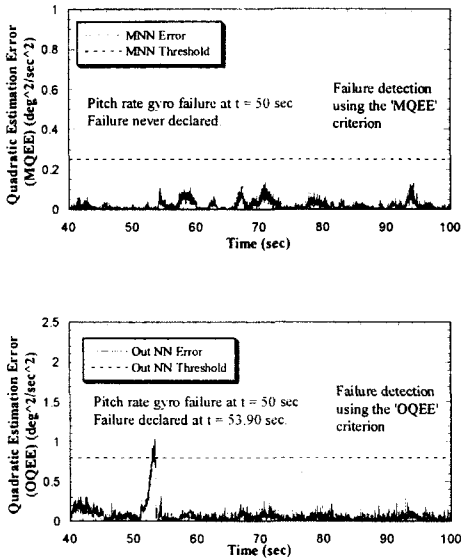


Fig. 2(a,b) Detection phase for the additive ramp-type pitch rate gyro failure (Type #4)

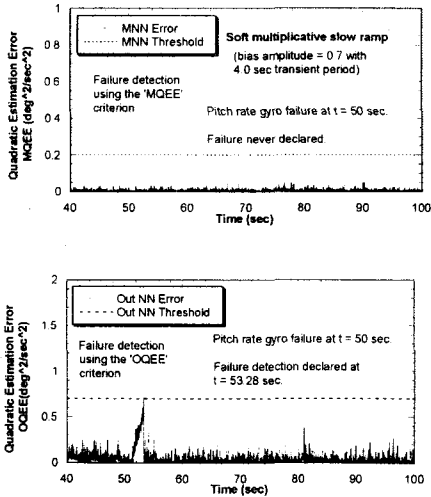


Fig. 3(a,b) Detection phase for the multiplicative ramp-type roll rate gyro failure (Type #4)

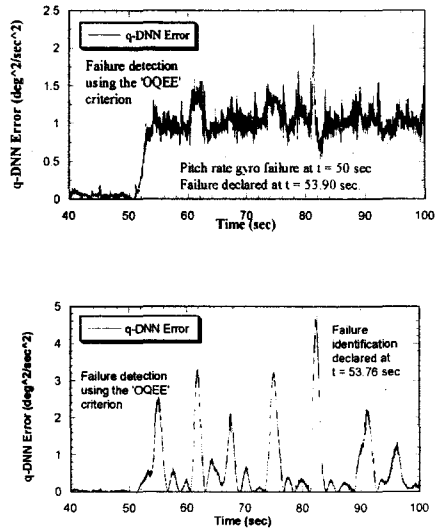


Fig. 4(a,b) Identification phase for the additive(a) & multiplicative(b) ramp-type pitch rate gyro failure (Type #4)

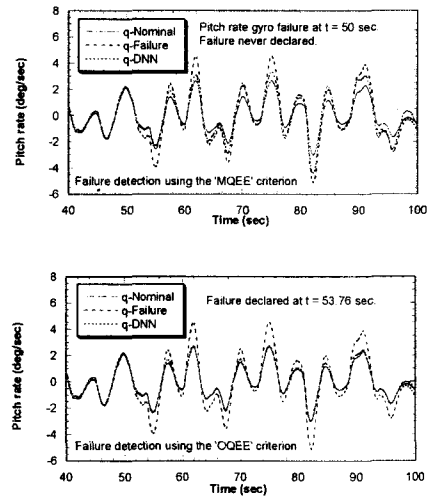


Fig. 5(a,b) Comparison of accommodation phase between two detection criterion for the multiplicative ramp-type pitch rate gyro failure (Type #4)

However, from Fig. 2(a) and 3(a) (Type#4), it can be seen that the MQEE criterion does not provide detection spike although there are some DNN errors following

pitch rate gyro failure, as shown Figs. 4(a, b). As a result, there is some decrease in the q-DNN's estimation accuracy in Fig. 5(a) since faulty measurements for q is continuously fed into the DNN's target value due to on-line learning process. Figs. 2(b) and 3(b) show that the SFD scheme is successful for the pitch rate gyro following sensor failure since the OQEE exceeded the predefined threshold during the observation period after sensor failure. As a result of successful detection phase, the time history of q-DNN is in good agreement with the nominal time history for pitch rate gyro, as shown in Fig. 5(b).

4. CONCLUSION

This paper has presented a neural network-based sensor failure detection, identification, and accommodation in a flight control system without physical redundancy in the sensors. This fault tolerant flight control system is based on the introduction of a main neural network and a set of decentralized on-line learning neural networks. Step-type and ramp-type transient failures of the pitch rate gyro were simulated and discussed for a model of a commercial transport airplane using two different detection parameters. As the results show, the quick failure detection is achieved by MQEE only for the step-type sensor failures while OQEE provides good performance for the ramp-type sensor failures, especially, for the small bias with slow ramp transient failure. Therefore, the combined detection scheme can trigger any variety of sensor failures that are not a characteristic of the nominal trend.

REFERENCES

1. Napolitano, M.R., Neppach, C. et. al., "Neural-Network-Based Scheme for Sensor Failure Detection, Identification, and Accommodation," *AIAA Journal of Guidance, Control, and Dynamics*, Vol. 18, No.6, pp 1280-1286, 1995.
2. Napolitano, M.R., Naylor, S. et.al., "On-Line Learning Nonlinear Direct Neurocontrollers for Restructurable Control Systems," *AIAA Journal of Guidance, Control, and Dynamics*, Vol.18, No.1, pp.170-176, 1995.
3. Wilsky, A.S., "Failure Detection in Dynamic Systems," *Agard LS-109, Neuilly sur Seine, France*, pp 2.1-2.14, 1980.
4. Kerr, T.H., "False Alarm and Correct Detection Probabilities over a Time Interval for Restricted Classes of Failure Detection Algorithms," *IEEE Transactions of Information Theory*, Vol. IT-28, No. 4, pp 619-631, 1982.
5. Napolitano, M.R., Chen, C.I., et. al., "Aircraft Failure Detection and Identification Using Neural Networks," *AIAA Journal of Guidance, Control, and Dynamics*, Vol. 16, No.6, pp 999-1009, 1993.
6. Windon, D.A., "Design and Comparison of Neural Network and Kalman Predictor Based Sensor Validation Schemes for Implementation on the NASA-Aurora Theseus Aircraft," Master Thesis, Department of Mechanical and Aerospace Engineering, West Virginia University, 1996.
7. Simpson, P.K., "Artificial Neural Systems: Foundations, Paradigms, Applications, and Implementations," Pergamon Press, New York, 1990.
8. Fausett, L.V., "Fundamentals of Neural Networks: Architectures, Algorithms, and Applications," Prentice Hall, Englewood Cliffs, 1994.
9. Chen, C.L., Nutter, R.S., "An Extended Back-Propagation Learning by Using Heterogeneous Processing Units," *Proceedings of International Joint Conference on Neural Networks*, Baltimore, Maryland, 1992.
10. Roskam, Jan, "Airplane Flight Dynamics and Automatic Flight Controls," Part I, Design, Analysis and Research Corporation, Lawrence, Kansas, 1995.